TLR8 deficiency leads to autoimmunity in mice

Olivier Demaria,[1,2,3] Philippe P. Pagni,[1,2,3] Stephanie Traub,[1,2,3] Aude de Gassart,[1,2,3] Nora Branzk,[1,2,3] Andrew J. Murphy,[4] David M. Valenzuela,[4] George D. Yancopoulos,[4] Richard A. Flavell,[5,6] and Lena Alexopoulou[1,2,3]

[1]Centre d'Immunologie de Marseille-Luminy, Université de la Méditerranée, Marseille, France. [2]INSERM U631, Marseille, France. [3]CNRS UMR6102, Marseille, France. [4]Regeneron Pharmaceuticals, Tarrytown, New York, USA. [5]Department of Immunobiology and [6]Howard Hughes Medical Institute, Yale University School of Medicine, New Haven, Connecticut, USA.

TLRs play an essential role in the induction of immune responses by detecting conserved molecular products of microorganisms. However, the function of TLR8 is largely unknown. In the current study, we investigated the role of TLR8 signaling in immunity in mice. We found that *Tlr8*$^{-/-}$ DCs overexpressed TLR7, were hyperresponsive to various TLR7 ligands, and showed stronger and faster NF-κB activation upon stimulation with the TLR7 ligand R848. *Tlr8*$^{-/-}$ mice showed splenomegaly, defective development of marginal zone (MZ) and B1 B cells, and increased serum levels of IgM and IgG2a. Furthermore, *Tlr8*$^{-/-}$ mice exhibited increased serum levels of autoantibodies against small nuclear ribonucleoproteins, ribonucleoprotein, and dsDNA and developed glomerulonephritis, whereas neither *Tlr7*$^{-/-}$ nor *Tlr8*$^{-/-}$*Tlr7*$^{-/-}$ mice showed any of the phenotypes observed in *Tlr8*$^{-/-}$ mice. These data provide evidence for a pivotal role for mouse TLR8 in the regulation of mouse TLR7 expression and prevention of spontaneous autoimmunity.

Introduction

TLRs, mammalian homologs of the *Drosophila* receptor Toll, detect evolutionarily conserved structures expressed by different groups of microbes and play a major role in the elimination of infections by coactivation of the immune system (1). TLRs are composed of an ectodomain of leucine-rich repeats, which are involved in ligand binding, a transmembrane domain, and a cytoplasmic Toll/IL-1 receptor (TIR) domain that interacts with TIR domain–containing adaptor molecules. The signaling pathways activated by different TLRs involve a family of 5 adaptor proteins, which couple to downstream protein kinases and ultimately lead to the activation of transcription factors such as NF-κB, MAPKs, and members of the IFN-regulatory factor family (2).

The family of TLRs consists of 10 members in humans (TLR1–TLR10) and 12 members in mice (TLR1–TLR9 and TLR11–TLR13). The mammalian TLRs that are located in the plasma membrane recognize bacterial membrane components, whereas the TLRs that detect nucleic acid–based ligands are predominately located within endosomal compartments (3). The nucleic acid–sensing TLRs include TLR3, TLR7, TLR8, and TLR9. TLR3 senses viral and synthetic double-stranded RNA, TLR7 recognizes viral single-stranded RNA (ssRNA) and synthetic imidazoquinoline compounds, and TLR9 detects unmethylated CpG containing DNA motifs, found in bacterial and viral DNA (3). Although TLR7 and TLR8 are phylogenetically very close, their natural ligand viral ssRNA stimulates human TLR7 and TLR8 and mouse TLR7, but not mouse TLR8, leading to the belief that TLR8 is biologically inactive in mice (4). However, recent studies have shown that TLR8 is dynamically expressed during mouse brain development and functions as a negative regulator of neurite outgrowth and an inducer of neuronal apoptosis (5). Moreover, stimulation of murine TLR8–transfected HEK293 cells with a combination of imidazoquinoline immune response modifiers and polyT oligonucleotides leads to NF-κB activation, which suggests that mouse TLR8 is functional (6). Upon ligand binding, most TLRs form homodimers; however, some ligands require TLR cooperation of 2 different TLRs in activating downstream signaling cascades. For example, TLR1/2 and TLR2/6 heterodimers are required for the detection of bacterial cell wall components (7–9).

TLRs are expressed on many cell types, including human and mouse DCs and B cells (1, 10, 11). The recognition of invading microbes by TLRs on DCs induces the activation and maturation of DCs, which instruct and support T cell activation and lead to cell-mediated adaptive immune response (12). Interaction between activated antigen-specific T cells and naive B cells promotes B cell expansion and differentiation, leading to a humoral immune response. Recent studies have shown that direct TLR-mediated activation of B cells is also required for eliciting humoral immune responses (13), although this has been challenged (14). However, TLR9 expression in B cells and not other antigen-presenting cells has been shown to be critical for the regulation of IgG isotype patterns (15). Moreover, different B cell subsets — including follicular, marginal zone (MZ), B1, and Peyer patch B cells — express multiple TLRs and have the ability to proliferate and secrete polyclonal antibodies to a variety of TLR agonists, even in the absence of DC activation or T cell help (11). Thus, splenic MZ B cells and B1 cells, which are located mainly in the peritoneal and pleural cavities, bridge innate and adaptive immunity by producing a rapid T cell–independent antibody response (16).

There is increasing evidence that TLRs can also recognize self-antigens released from damaged or stressed host tissue and that such recognition can lead to the development of autoimmune disease, including SLE (17). Most interest has focused on the nucleic acid–sensing TLRs TLR3, TLR7, and TLR9 (18, 19). In humans, the etiology of SLE is unknown, but inherited genes, viruses, ultraviolet light, and certain medications may all play some role. SLE patients experience kidney dysfunction leading to renal failure and a wide and variable range of symptoms, including arthritis, skin rashes, fever, and brain inflammation. The association of the nucleic acid–sensing TLRs with lupus originates mainly from mouse models, where activation of any of these receptors in vivo

Conflict of interest: A.J. Murphy, D.M. Valenzuela, and G.D. Yancopoulos are employed by Regeneron Pharmaceuticals.

Citation for this article: *J Clin Invest.* 2010;120(10):3651–3662. doi:10.1172/JCI42081.

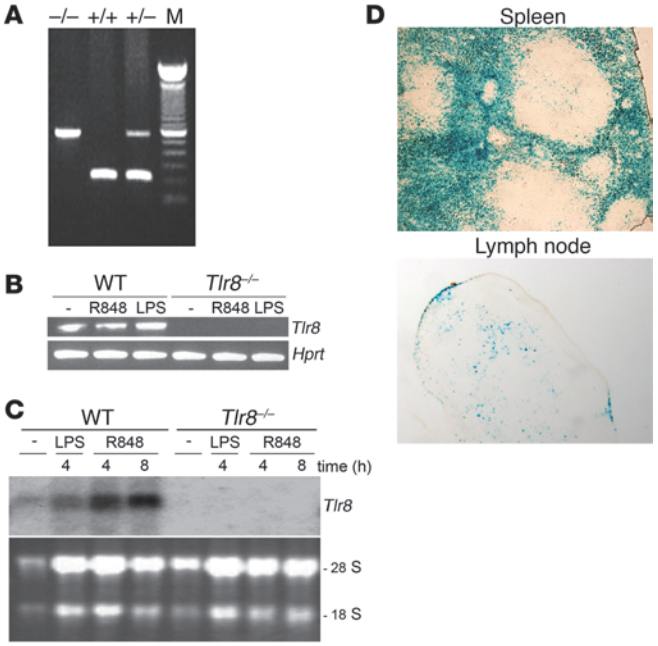

Figure 1
Targeted disruption of the mouse *Tlr8* gene. (**A**) PCR analysis of mouse genomic DNA with specific primers gave a 240-bp band for $Tlr8^{+/+}$ mice, a 589-bp band for $Tlr8^{-/-}$ mice, and both bands for $Tlr8^{+/-}$ mice. M, molecular weight marker (100-bp DNA ladder; Invitrogen). (**B**) Expression of *Tlr8* and *Hprt* mRNA by WT and $Tlr8^{-/-}$ BMDCs either untreated or stimulated with 50 nM R848 or 1 ng/ml LPS for 4 hours, as determined by RT-PCR. (**C**) Northern blot analysis of RNA from untreated, 1 ng/ml LPS–, or 50 nM R848–stimulated WT and $Tlr8^{-/-}$ BMDCs. Ethidium bromide staining after RNA transfer to the membrane is included as control (bottom). (**D**) Reporter gene expression (LacZ reporter, blue) in spleen and mesenteric lymph node sections from $Tlr8^{-/-}$ mice. (**A**–**D**) Data are representative of 2–4 independent experiments.

augments nephritis (20–22). Furthermore, in the MRL/lpr lupus mouse model, deletion of the *Tlr7* gene was shown to be protective and to reduce the amount of antibodies against RNA-related antigens, whereas *Tlr9* deficiency led to exacerbation of the autoimmune disease (23). In addition, mice bearing the Y chromosome–linked autoimmune accelerating (Yaa) locus provide a good example of how important it is to control the expression of TLRs. The Yaa locus harbors 17 different genes, including *Tlr7*, and produces an impressive acceleration of autoimmunity when bred to several murine models of lupus. Interestingly, recent studies have shown that the Yaa locus in part mediates the autoimmune phenotype via duplication of TLR7 (24–27).

Mammalian TLR8 is one of the least-studied members of the TLR family. To investigate the role of TLR8 in immunological processes, we generated TLR8-deficient ($Tlr8^{-/-}$) mice by gene targeting. In the absence of TLR8, DCs showed overexpression of TLR7 that was accompanied by increased responses to various TLR7 ligands and NF-κB activation. TLR8 deficiency in mice led to reduced numbers of MZ and peritoneal cavity B1 B cells and increased levels of circulating IgM and IgG2a antibodies. Experiments with BM chimeras revealed that MZ B cells and B1 cell phenotypes were associated with the absence of TLR8 in radiosensitive hematopoietic cells, but not in radioresistant structural cells. In addition, TLR8 deficiency led to elevated levels of IgG autoantibodies to ribonucleoprotein (RNP), small nuclear RNP (smRNP), and dsDNA and to glomerulonephritis with more abundant deposits of immune complexes in the glomeruli of $Tlr8^{-/-}$ mice. We conclude that murine TLR8 plays an important role in controlling TLR7 expression, which is critical for promoting autoantibody production and lupus disease development.

Results

Generation and characterization of $Tlr8^{-/-}$ mice. To investigate the function of TLR8 in vivo, $Tlr8^{-/-}$ mice (Figure 1A) were generated by a high-throughput, automated approach (see Methods and ref. 28). The expression of *Tlr8* mRNA was abrogated in $Tlr8^{-/-}$, but not WT, BM-derived DCs (BMDCs), as assessed by RT-PCR and Northern blot analysis (Figure 1, B and C). $Tlr8^{-/-}$ mice were born at the expected Mendelian ratio; had normal growth, size, fertility, and life span; and showed no obvious developmental or behavioral abnormalities. To study the natural expression of *Tlr8*, the expression of the lacZ reporter gene that was introduced under the TLR8 promoter in $Tlr8^{-/-}$ mice was determined by β-galactosidase assay on cryostat organ sections. In the spleen, the site of TLR8 expression was confined in few cells in the T cell area of the white pulp, consistent with the location of DCs, while there was widespread expression in the red pulp, which is rich in macrophages (Figure 1D). Within the mesenteric lymph nodes, the site of TLR8 expression was confined to the perifollicular regions, where DCs are also located (Figure 1D).

To determine the functional role of TLR8, we analyzed the responses of $Tlr8^{-/-}$ cells to various TLR ligands. $Tlr8^{-/-}$ and WT BMDCs, BM-derived macrophages (BMMs), and total splenocytes were stimulated with various doses of TLR7 ligand R848, TLR3 and TLR7 ligand polyA:U, TLR9 ligand CpG, TLR3 ligand polyI:C, and TLR4 ligand LPS. After 20 hours, the culture supernatants were collected, and the protein levels of IL-6, IL-12p40, and TNF were assessed by ELISA. The production of IL-6, IL-12p40, and TNF in response to R848 and polyA:U was considerably higher in $Tlr8^{-/-}$ than in WT BMDCs, whereas responses to CpG, polyI:C, and LPS were similar between WT and $Tlr8^{-/-}$ BMDCs (Figure 2A). However, WT and $Tlr8^{-/-}$ BMMs and total splenocytes showed similar cytokine responses to R848, CpG, and LPS (Supplemental Figure 1; supplemental material available online with this article; doi:10.1172/JCI42081DS1, and data not shown). Moreover, upon R848 stimulation, $Tlr8^{-/-}$ BMDCs showed higher production of *Ifnb* at the mRNA level than did WT cells (Figure 2B).

To further study whether the defect in the $Tlr8^{-/-}$ BMDCs is restricted to the TLR7 ligands R848 and polyA:U, we compared the responses of WT and $Tlr8^{-/-}$ BMDCs to a panel of known TLR7 ligands, such as TLR7/8 ligand CL075, which acts as a stronger ligand for human TLR8 than for human TLR7; TLR7/8 ligand CL097; and TLR7/8 ligand ssRNA-DR/LyoVec, composed of ssRNA complexed with cationic lipid LyoVec to facilitate its uptake by the cells. We found that $Tlr8^{-/-}$ BMDCs produced markedly higher amounts of IL-12p40 compared with WT cells in response to all the TLR7 ligands tested (Supplemental Figure 2). Moreover, we assessed the effect of delivering R848 or polyA:U intracellularly using lipofectamine, a reagent for nucleic acid transfer. Although the responses of WT and $Tlr8^{-/-}$ BMDCs were higher compared with non–lipofectamine-treated cells, the $Tlr8^{-/-}$ cells were again higher producers than WT controls (data not shown). Next, we evaluated the activation of $Tlr8^{-/-}$ and WT BMDCs based on the

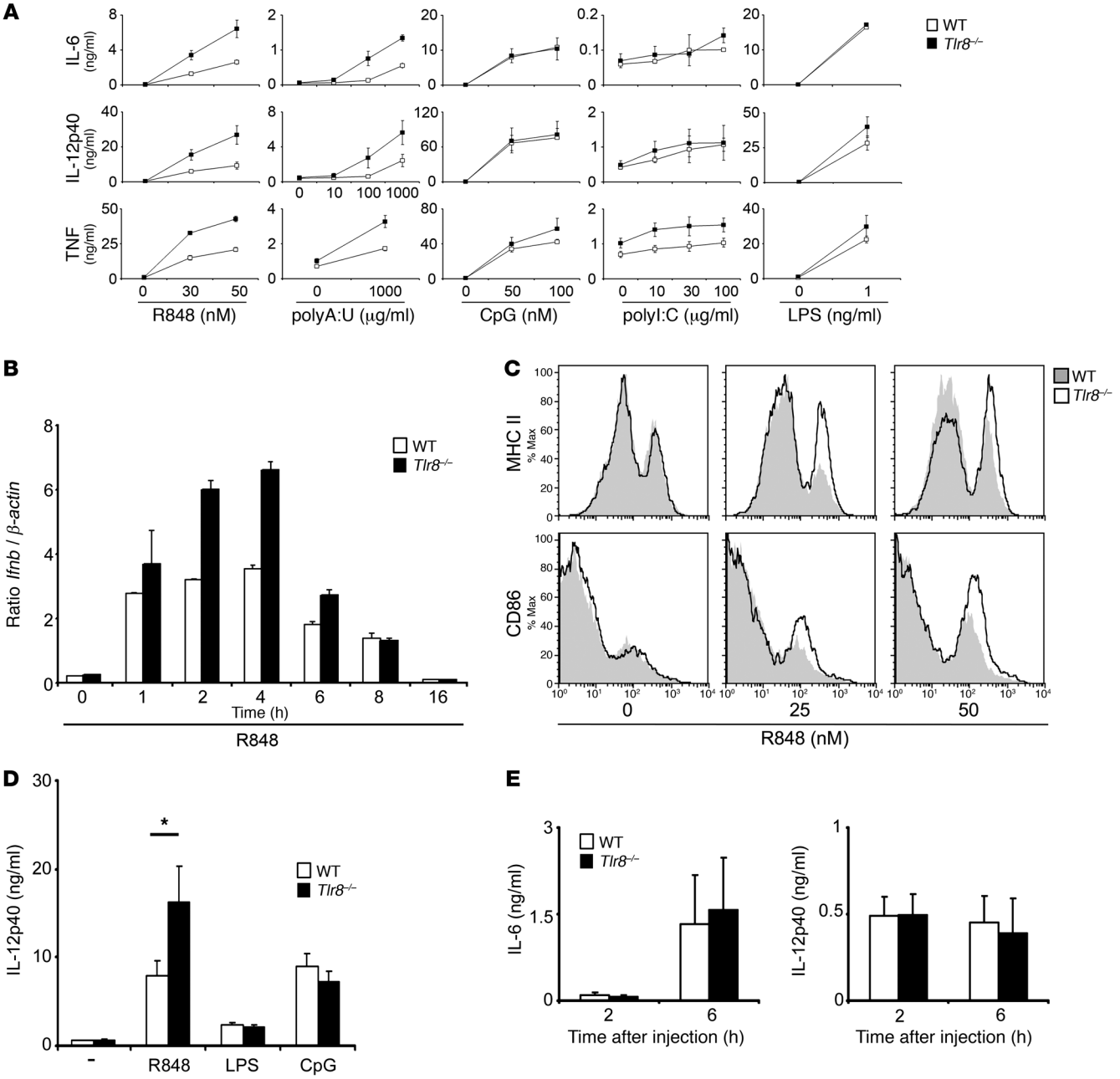

Figure 2

Enhanced responses to TLR7 ligands by *Tlr8*$^{-/-}$ DCs. (**A**) BMDCs from WT and *Tlr8*$^{-/-}$ mice were stimulated with the indicated amounts of R848, polyA:U, CpG, polyI:C, and LPS. After 20 hours, the concentrations of IL-6, IL-12p40, and TNF in the culture supernatants were assessed by ELISA. (**B**) WT and *Tlr8*$^{-/-}$ BMDCs were left untreated or stimulated for the indicated times with 50 nM R848. Total RNA was extracted from the cells, and expression of *Ifnb* was assessed by Q-PCR. (**C**) WT and *Tlr8*$^{-/-}$ BMDCs were left untreated or stimulated with the indicated amounts of R848 for 16 hours, and cell surface expression of MHCII and CD86 was analyzed by flow cytometry on gated CD11c^{+} cells. (**D**) WT and *Tlr8*$^{-/-}$ CD11c^{+} splenic cells were isolated by magnetic-activated cell sorting, then left unstimulated or stimulated for 16 hours with 30 nM R848, 10 ng/ml LPS, or 30 nM CpG. The production of IL-12p40 in the culture supernatants was assessed by ELISA. *$P < 0.05$. (**E**) WT and *Tlr8*$^{-/-}$ mice (8 weeks old) were injected i.p. with 100 μl of 10 μM R848. Sera were collected 2 or 6 hours later, and serum levels of IL-6 and IL-12p40 were determined by ELISA. (**A**, **D**, and **E**) Data are mean ± SD of 3–4 (**A** and **D**) or 8–10 (**E**) mice per group and are representative of 2–5 independent experiments. (**B**) Data are mean ± SD of duplicates and are representative of 2 independent experiments.

expression of CD86 and MHC class II (MHCII). Untreated WT and *Tlr8*$^{-/-}$ cells had similar levels of CD86 and MHCII; however, upon stimulation with 25 or 50 nM R848, *Tlr8*$^{-/-}$ BMDCs showed higher augmentation of the expression of these surface molecules compared with WT cells (Figure 2C). Moreover, we compared the responses of WT and *Tlr8*$^{-/-}$ splenic DCs and found that TLR8 deficiency led to higher IL-12p40 production upon stimulation with R848, but not with LPS or CpG (Figure 2D). Next, *Tlr8*$^{-/-}$ and

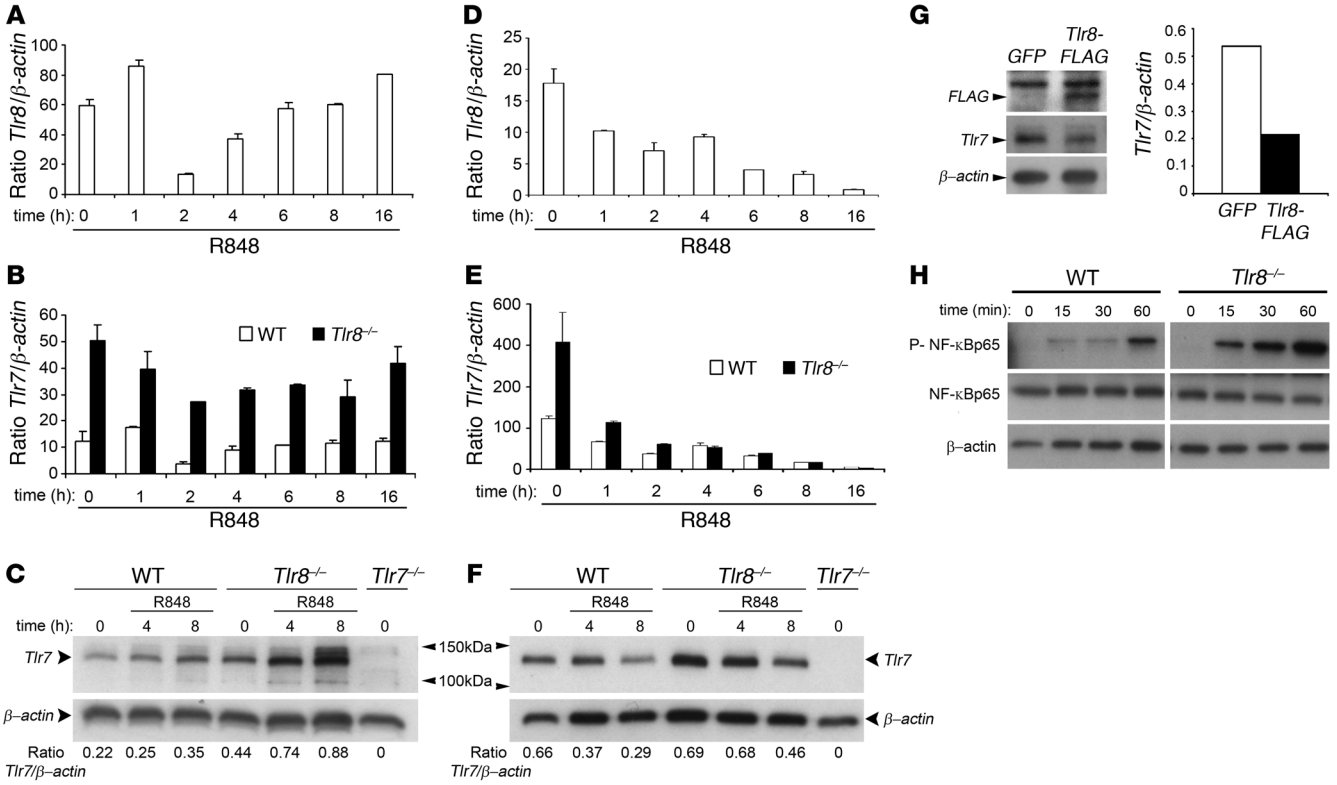

Figure 3

Increased TLR7 expression and NF-κB activation in *Tlr8*$^{-/-}$ BMDCs. WT and *Tlr8*$^{-/-}$ BMDCs were left untreated or stimulated with 50 nM (**A** and **B**) or 100 nM (**C** and **H**) R848 for the indicated times. Total mRNA was extracted from the cells, and the expression of (**A**) *Tlr8* or (**B**) *Tlr7* was assessed by Q-PCR. Total protein lysates were prepared, and (**C**) the expression of *Tlr7* and β-*actin* were assessed at 0, 4, and 8 hours after stimulation, or (**H**) phosphorylation of NF-κBp65 was determined by Western blot. Total NF-κBp65 and β-actin were used as loading controls. (**D**–**F**) WT and *Tlr8*$^{-/-}$ BMMs were left untreated or stimulated with 50 nM R848. At the indicated time points, either total mRNA was extracted from the cells and the expression of (**D**) *Tlr8* and (**E**) *Tlr7* was assessed by Q-PCR, or (**F**) total protein lysates were prepared, and the expression of *Tlr7* and β-*actin* were assessed by Western blot. (**G**) *Tlr8*$^{-/-}$ BMDCs were transfected with 50 pmol *Tlr8-FLAG* or *GFP* mRNA. 5 hours later, cells were harvested, total protein lysates were prepared, and the expression of *Tlr7*, *Tlr8-FLAG*, and β-*actin* were assessed by Western blot. The *Tlr7*/β-*actin* ratio is shown at right. (**A**, **B**, **D**, and **E**) Data are mean ± SD of duplicates and are representative of 2–3 independent experiments. (**C**, **F**, **G**, and **H**) Data are representative of 3–5 (**C**, **F**, and **H**) or 2 (**G**) independent experiments.

WT mice were injected i.p. with R848, and their sera were collected 2 and 6 hours later. *Tlr8*$^{-/-}$ mice exhibited IL-6 and IL-12p40 production in their sera similar to that of WT controls (Figure 2E). Thus, TLR8 deficiency in DCs, but not in macrophages or total splenocytes, led to increased response to TLR7 ligands.

To further confirm that the increased response of *Tlr8*$^{-/-}$ DCs to R848 stimulation is caused by the absence of TLR8 and not by off-target effects, since TLR7 is located in the same chromosome as TLR8 and only 70 kb apart, we tested whether the addition of a functional *Tlr8* gene restores the phenotype in *Tlr8*$^{-/-}$ DCs. Indeed, *Tlr8* expression in *Tlr8*$^{-/-}$ BMDCs substantially reduced their hyperresponsiveness to R848 stimulation, but the response to the TLR9 ligand CpG was unaltered (Supplemental Figure 3).

Increased TLR7 expression and NF-κB activation in BMDCs in the absence of TLR8. Quantitative real-time PCR (Q-PCR) analysis revealed expression of murine TLR8 in WT BMDCs; upon stimulation with R848, *Tlr8* mRNA levels were dramatic downregulated at 2 hours, and expression returned to normal levels after 6 hours (Figure 3A), suggestive of transient negative regulation of TLR8 expression. To further explore this phenomenon, we stimulated BMDCs with IFN-γ and TNF-α and found that *Tlr8* mRNA expression was affected (Supplemental Figure 4, A and B), which suggests that regulation of TLR8 expression depends on the activation status of the cell. We next examined whether the higher cytokine production in response to TLR7 ligands in *Tlr8*$^{-/-}$ BMDCs correlates with altered TLR7 expression. *Tlr8*$^{-/-}$ and WT BMDCs were left untreated or were stimulated with R848 for different times. In WT cells, the kinetics of *Tlr7* mRNA expression were similar to those of *Tlr8*, with a dramatic downregulation at 2 hours and restoration of normal levels by 6 hours (Figure 3B). However, untreated *Tlr8*$^{-/-}$ BMDCs expressed approximately 4 times more *Tlr7* mRNA than did WT cells, and upon R848 stimulation, *Tlr8*$^{-/-}$ BMDCs always showed higher expression of *Tlr7* compared with WT cells (2–6 times; Figure 3B). To determine whether this difference at the mRNA level is also reflected at the protein level, the expression of TLR7 protein was assessed by Western blot on total protein lysates from WT and *Tlr8*$^{-/-}$ BMDCs. TLR8 deficiency was associated with higher expression of the TLR7 protein in both untreated and R848-stimulated DCs (Figure 3C). Next, we examined the expression of TLR8 and TLR7 in macrophages. *Tlr8* and *Tlr7* mRNAs

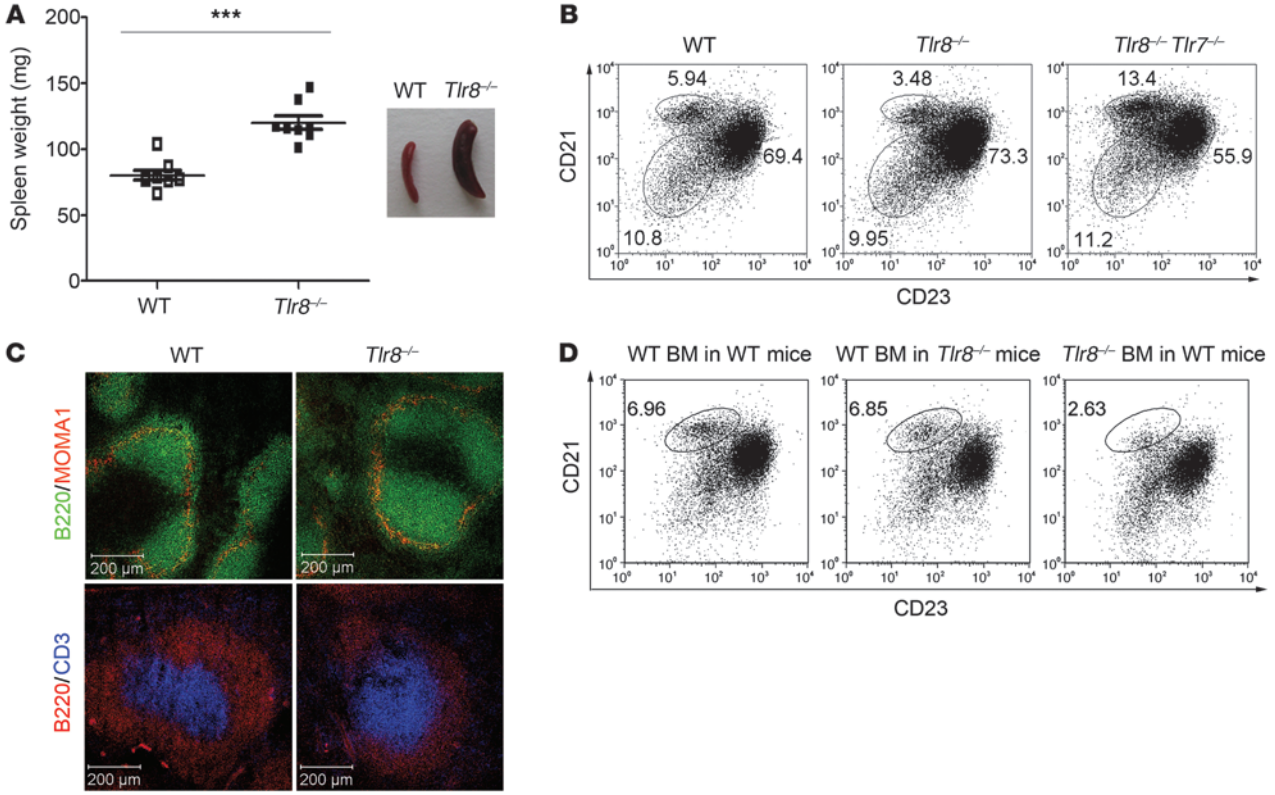

Figure 4

Defect of MZ B cells in *Tlr8*$^{-/-}$ mice. (**A**) Spleen weight and size of 8-week-old male WT and *Tlr8*$^{-/-}$ mice. Each point represents the value obtained from 1 mouse; horizontal bars denote mean values. ***$P < 0.001$. (**B**) Erythrocyte-depleted splenocytes from 6-month-old WT, *Tlr8*$^{-/-}$, and *Tlr8*$^{-/-}$*Tlr7*$^{-/-}$ mice were analyzed by flow cytometry for the expression of CD19, CD21, and CD23. Profiles using anti-CD21 and anti-CD23 were performed on CD19^{+} gated cells. Numbers denote the percentage of immature B cells (CD21^{-}CD23^{-}), follicular B cells (CD21^{int}CD23^{hi}) and MZ B cells (CD21^{hi}CD23$^{lo/-}$) in the indicated circles. (**C**) Spleen sections from WT or *Tlr8*$^{-/-}$ mice stained for MOMA1 (red) and B220 (green), or for B220 (red) and CD3 (blue). Scale bars: 200 μm. (**D**) BM cells (2×10^6 cells) from WT or *Tlr8*$^{-/-}$ mice were transferred i.v. into lethally irradiated WT or *Tlr8*$^{-/-}$ mice. After 6–8 weeks, splenocytes were analyzed by flow cytometry for the presence of MZ B cells. (**A**) Data are representative of 3 independent experiments with 5–9 mice per group. (**B**) Data are representative of 5 independent experiments with 3–4 mice per group. (**C** and **D**) Data are representative of 2 independent experiments with 3 mice per group.

were expressed in WT BMMs; upon stimulation with R848, expression of both was downregulated and almost totally abolished by 16 hours (Figure 3, D and E). Untreated *Tlr8*$^{-/-}$ BMMs expressed higher levels of *Tlr7* mRNA than did WT cells, but upon stimulation with R848, this difference was dramatically diminished: by 4 hours after stimulation, both *Tlr8*$^{-/-}$ and WT BMMs expressed similar levels of *Tlr7* mRNA (Figure 3E). At the protein level, untreated WT and *Tlr8*$^{-/-}$ BMMs expressed similar levels of TLR7, and although *Tlr8*$^{-/-}$ cells showed higher expression of TLR7 at 4 hours after R848 stimulation, this difference was reduced by the 8-hour time point (Figure 3F). Thus, in untreated DCs, but not macrophages, TLR8 deficiency correlated with higher expression of TLR7 protein, and this difference in TLR7 expression further increased upon activation with R848. To further confirm the dose-response relationship between TLR8 and TLR7 expression, we evaluated the levels of TLR7 in *Tlr8*$^{+/+}$*Tlr7*$^{+/+}$ (WT), *Tlr8*$^{-/-}$*Tlr7*$^{+/+}$ (*Tlr8*$^{-/-}$), *Tlr8*$^{-/-}$*Tlr7*$^{+/-}$, and *Tlr8*$^{+/+}$*Tlr7*$^{+/-}$ (*Tlr7*$^{+/-}$) BMDCs. We found that TLR7 expression in *Tlr8*$^{-/-}$*Tlr7*$^{+/-}$ DCs, at both the RNA and the protein levels, was lower than in *Tlr8*$^{-/-}$ cells and higher than in *Tlr7*$^{+/-}$ cells (Supplemental Figure 5, A and B), suggestive of TLR8-mediated regulation of TLR7 expression in DCs.

In addition, we investigated whether expression of TLR8 in *Tlr8*$^{-/-}$ BMDCs affects TLR7 protein levels. *Tlr8*$^{-/-}$ BMDCs were transfected with *Tlr8-FLAG* or *GFP* mRNA, and the expression of TLR7 and TLR8 was detected using antibodies against TLR7 and FLAG, respectively. Expression of TLR8 in *Tlr8*$^{-/-}$ BMDCs led to a dramatic reduction in the expression of TLR7 compared with cells transfected with GFP (Figure 3G), which suggests that TLR8 expression leads to reduced expression of the TLR7 protein.

Signaling via TLRs occurs through the recruitment of the adaptor molecule MyD88 and/or Toll/IL-1 receptor domain–containing adaptor inducing IFN-β (TRIF) and leads to activation of NF-κB and MAPKs (2). We therefore analyzed R848-induced NF-κB and MAPK activation by Western blot analysis in *Tlr8*$^{-/-}$ cells. R848 stimulation of *Tlr8*$^{-/-}$ BMDCs showed substantially faster and stronger phosphorylation of NF-κBp65 compared with WT cells (Figure 3H). However, degradation of IκBα and phosphorylation of IκBα, JNK, ERK1/2, and p38 were similar in WT and *Tlr8*$^{-/-}$ cells (Supplemental Figure 6).

Defect of MZ B cells in Tlr8$^{-/-}$ *mice.* We noticed that *Tlr8*$^{-/-}$ mice had exacerbated splenomegaly compared with sex- and age-matched WT controls (Figure 4A and Table 1). Flow cytometric analysis of various

Table 1
Frequency of splenic cell subsets in WT and *Tlr8*$^{-/-}$ mice

	WT	*Tlr8*$^{-/-}$
CD11b^{+}	10.4 ± 0.3	10.9 ± 0.7
Resident monocyte (CD11b^{+}GR-1^{lo})	75.6 ± 3.1	74.8 ± 1.6
Inflammatory monocyte (CD11b^{+}GR-1^{int})	7.3 ± 0.7	7.98 ± 0.4
Neutrophil (CD11b^{+}GR-1^{hi})	8.5 ± 2.2	9.9 ± 1.7
CD11c^{+}	3.9 ± 0.5	5.1 ± 0.4^{A}
Plasmacytoid DC (B220^{+}CD11c^{lo}Ly6C^{hi})	10.5 ± 1	9.5 ± 0.5
DC (B220^{-}CD11c^{hi}Ly6C^{-})	42.4 ± 1.7	35 ± 3.6^{A}
CD3^{+}	31.1 ± 2.2	29.7 ± 2.5
CD3^{+}CD4^{+}CD8^{-}	39.6 ± 2.8	37.2 ± 1.4
CD3^{+}CD4^{-}CD8^{+}	29.3 ± 2.3	29.3 ± 0.2
CD19^{+}	50.1 ± 2.6	60 ± 2.1^{B}
Follicular B (CD19^{+}CD23^{+}CD21^{-})	74.6 ± 1.5	76 ± 1
MZ B (CD19^{+}CD23^{-}CD21^{+})	7.1 ± 0.5	3.4 ± 0.7^{B}
Immature (CD19^{+}CD23^{-}CD21^{-})	14.6 ± 1.44	17.4 ± 1.6

Data are from 4.5-month-old female WT and *Tlr8*$^{-/-}$ mice. All values denote percentages (mean ± SD). Total spleen cell counts were 152 × 10^{6} ± 16.4 × 10^{6} for WT and 244 × 10^{6} ± 26.1 × 10^{6} for *Tlr8*$^{-/-}$ ($P < 0.01$). $^{A}P < 0.05$ versus WT. $^{B}P < 0.01$ versus WT.

splenic cell compartments showed that *Tlr8*$^{-/-}$ mice had a MZ defect and the CD11c^{+} population was expanded (Figure 4B and Table 1), similar to previous findings in transgenic mice overexpressing TLR7 (24). The MZ defect was further confirmed by the reduction of CD1d^{hi} cells among IgM^{hi}IgD^{lo} B lymphocytes, a characteristic trait of MZ B cells (data not shown). The percentages of splenic immature and follicular B cells, and CD4^{+} and CD8^{+} T cells, were similar in WT and *Tlr8*$^{-/-}$ mice (Figure 5B and Table 1), and no spontaneous activation was observed on B and T lymphocytes, as evaluated by CD69 and CD86 expression (Supplemental Figure 7A and data not shown). Furthermore, the myeloid progenitor fractions of the BM and thymic development was found to be normal, as assessed by FACS analysis (Supplemental Figure 7, B and C). In agreement with the flow cytometric results, the characteristic rim of B220^{+} MZ B cells peripheral to follicles, which lies external to the ring of metallophilic macrophages (MOMA1^{+}), was dramatically reduced in spleens derived from *Tlr8*$^{-/-}$ mice relative to WT controls (Figure 4C). However, histological examination of *Tlr8*$^{-/-}$ spleens showed normal microanatomic structures, containing T cell areas and B cell follicles (Figure 4C). These results confirmed the reduction of MZ B cells in *Tlr8*$^{-/-}$ mice despite normal follicular architecture. In order to determine whether the reduced MZ B cell phenotype we observed in *Tlr8*$^{-/-}$ mice correlates with overexpression of TLR7, we also assessed the MZ B cell population in *Tlr8*$^{-/-}$*Tlr7*$^{-/-}$ and *Tlr8*$^{-/-}$ mice. We observed a substantial increase of the MZ B cell population in *Tlr8*$^{-/-}$*Tlr7*$^{-/-}$ mice compared with WT controls, and this increase was accompanied by a reduction in the follicular B cell population (Figure 4B). In addition, *Tlr8*$^{-/-}$*Tlr7*$^{+/-}$ mice showed an intermediate MZ phenotype compared with *Tlr8*$^{-/-}$ and *Tlr8*$^{-/-}$*Tlr7*$^{-/-}$ mice, since the percentage of the MZ B cells was 2 times higher than in *Tlr8*$^{-/-}$ mice and 2 times lower than in *Tlr8*$^{-/-}$*Tlr7*$^{-/-}$ mice (Supplemental Figure 5C). Thus, TLR8 affects TLR7 expression and plays an important role in the development of a normal MZ B cell population.

Next, we examined the expression of TLR7 and TLR8 in MZ and follicular B cells by Q-PCR. Both MZ and follicular B cells from WT mice were expressing *Tlr7* mRNA, in accordance with previously published studies (10, 11), and TLR7 expression was at least 2 times higher in *Tlr8*$^{-/-}$ cells (Supplemental Figure 8A). When we tested the expression of TLR8 by Q-PCR in WT MZ B cells, we were unable to detect any *Tlr8* mRNA, in accordance with previously published data (10, 11). However, by classical PCR, we found that, indeed, both MZ and follicular B cells of WT mice expressed TLR8, as was the case for WT BMDCs and BMMs, whereas TLR8 expression was absent in *Tlr8*$^{-/-}$ BMDCs (Supplemental Figure 8B). We further compared the ability of WT and *Tlr8*$^{-/-}$ MZ B cells to respond to R848, and found that both genotypes produced similar levels of IL-6 upon R848 and CpG stimulation (Supplemental Figure 8C). Moreover, they showed similar expression of the activation markers CD86 and CD69 and the chemokine receptors CXCR5 and CXCR4 (Supplemental Figure 8D and data not shown). Thus, although MZ B cells expressed both TLR7 and TLR8, and we observed higher expression of TLR7 in *Tlr8*$^{-/-}$ than WT cells, *Tlr8*$^{-/-}$ MZ B cells were not hyperresponsive to R848 stimulation.

Requirement of TLR8 expression by BM-derived cells for normal MZ B cell population numbers. To determine whether the impaired MZ B cell development in *Tlr8*$^{-/-}$ mice results from a defect on the BM-derived cell population or a defect in the stromal microenvironment that supports the differentiation of these specialized cells, we performed reciprocal BM reconstitution experiments between WT and *Tlr8*$^{-/-}$ mice. The transfer of BM cells from WT mice into irradiated *Tlr8*$^{-/-}$ mice efficiently reconstituted MZ B cells (7.1% ± 1.6%; mean ± SD of 6 mice), as documented by flow cytometric analysis (Figure 4D). The extent of the MZ B cell development observed in these mice was comparable to that observed in irradiated WT mice reconstituted with WT BM cells (6.6% ± 0.7%; mean ± SD of 5 mice). In contrast, MZ B cells were poorly developed in irradiated WT mice reconstituted with *Tlr8*$^{-/-}$ BM cells (2.6% ± 0.7%; mean ± SD of 6 mice; Figure 4D). Thus, WT BM cells gave rise to normal numbers of MZ B cells in the absence of TLR8 expression by radioresistant stromal cells. In contrast, *Tlr8*$^{-/-}$ BM cells were unable to give rise to normal numbers of MZ B cells in the presence of WT radioresistant stromal cells.

Defect of B1 B cell development in Tlr8$^{-/-}$ *mice.* B1 B cells represent an important cell population for the production of natural antibodies and for antibacterial Ig responses and share a number of properties with MZ B cells. Thus, we tested whether the absence of TLR8 affects the B1 B cell population. Most B1 B cells reside in the peritoneal and pleural cavities; they include B1a cells, which express CD5, and B1b cells, which are CD5^{lo}. FACS analysis showed that the relative percentage of B1a B cells (B220^{lo}CD5^{int}) in the peritoneal cavity of *Tlr8*$^{-/-}$ mice was dramatically reduced by about 3-fold compared with that in WT mice (*Tlr8*$^{-/-}$, 9.3% ± 2.0%; WT, 29.1% ± 4.8%; mean ± SD of 3 mice; Figure 5A). Moreover, there was a similar reduction in the percentage of B1b B cells (B220^{lo}CD5^{lo}) in *Tlr8*$^{-/-}$ mice (*Tlr8*$^{-/-}$, 5.4% ± 2.3%; WT, 17.6 ± 3.1; mean ± SD of 3 mice; Figure 5A). Analysis of the B2 B cell population (B220^{hi}CD5^{-}) of the peritoneal cavity showed an increased percentage of these cells in *Tlr8*$^{-/-}$ compared with WT mice (Figure 5A). Similar differences were observed in the absolute numbers of B1a, B1b, and B2 B cells in *Tlr8*$^{-/-}$ versus WT mice (data not shown).

Analysis of the B1 B cell population in irradiated WT or *Tlr8*$^{-/-}$ recipient mice reconstituted with WT or *Tlr8*$^{-/-}$ BM cells revealed that the B1 B cell defect in *Tlr8*$^{-/-}$ mice was BM-derived cell–autonomous (Figure 5B). Therefore, TLR8 deficiency in BM-derived cells impairs the development and/or maintenance of the B1 B cell subset.

TLR8 deficiency is sufficient to induce systemic autoimmunity. Overexpression of TLR7 in several mouse strains has previously been

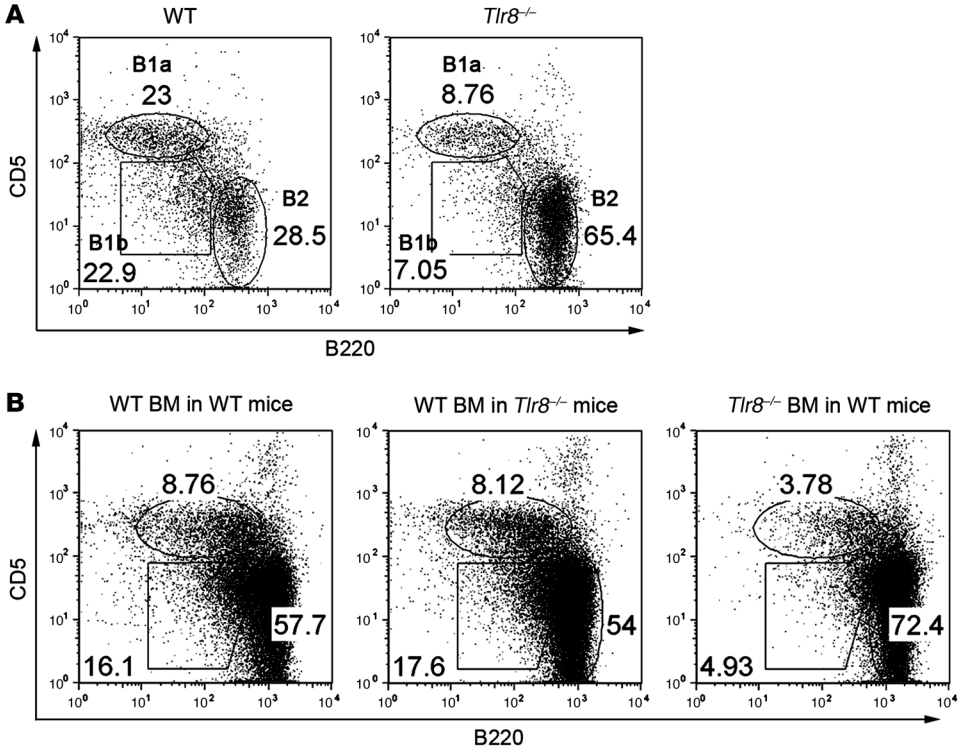

Figure 5
Reduced numbers of B1 B cells in *Tlr8*$^{-/-}$ mice. Peritoneal cavity cells from (**A**) 11-week-old WT and *Tlr8*$^{-/-}$ mice or (**B**) lethally irradiated WT and *Tlr8*$^{-/-}$ mice reconstituted i.v. with 2 × 10^6 WT or *Tlr8*$^{-/-}$ BM cells were analyzed by flow cytometry for expression of CD19, B220, and CD5. Shown are percent B1a (B220^{lo}CD5^{int}), B1b (B220^{lo}CD5^{lo}), and B2 (B220^{hi}CD5^{-}) B cells on CD19$^+$ gated cells of the peritoneal cavity. Data are representative of 2–3 independent experiments with 3 mice per group.

shown to promote autoantibody production and pathological disease associated with lupus (24–26). To determine whether the augmented TLR7 expression we observed in *Tlr8*$^{-/-}$ mice correlates with autoimmunity, serum levels of IgM and IgG isotypes were assessed in 3-month-old WT, *Tlr8*$^{-/-}$, and *Tlr7*$^{-/-}$ mice by ELISA. Levels of IgM and IgG2a were significantly higher, whereas levels of total IgG, IgG2b, and IgG3 were similar, in *Tlr8*$^{-/-}$ compared with WT mice (Figure 6). In contrast, *Tlr7*$^{-/-}$ mice showed significantly lower levels of IgM, total IgG, IgG1, and IgG2a, but similar levels of IgG2b and IgG3, compared with WT mice (Figure 6). *Tlr8*$^{-/-}$ mice also had significantly lower levels of IgG1 compared with control mice (Figure 6). Next, we assessed the levels of IgG autoantibodies against smRNP, RNP, and dsDNA and found that the titers of all 3 autoantibodies were significantly increased in *Tlr8*$^{-/-}$ versus WT sera (Figure 7A). To further study the role of TLR8 in the generation of antinuclear Abs (ANAs), we used the fluorescent ANA assay on Hep-2 cells as a sensitive detection method for Abs to both RNA- and DNA-containing autoantigens. Strikingly, *Tlr8*$^{-/-}$ sera were strongly positive for ANAs, whereas WT mice had weak ANA staining and both *Tlr7*$^{-/-}$ and *Tlr8*$^{-/-}$*Tlr7*$^{-/-}$ mice were negative (Figure 7B). Moreover, *Tlr8*$^{-/-}$*Tlr7*$^{+/-}$ sera showed ANA titers lower than those in *Tlr8*$^{-/-}$ samples (Supplemental Figure 5D). Since we detected increased autoantibody production in *Tlr8*$^{-/-}$ sera, we analyzed the B cells in these mice and found that the B220^{lo}CD138$^+$ population, most likely representing Ab-producing cells, was increased (Supplemental Figure 8E). Immunostaining and fluorescence microscopy of WT, *Tlr8*$^{-/-}$, and *Tlr7*$^{-/-}$ kidneys revealed that glomerular deposition of IgM, IgG, and complement component C3 were substantially greater in *Tlr8*$^{-/-}$ mice than in WT controls at 4 months of age, whereas *Tlr7*$^{-/-}$ mice showed diminished deposition of IgM, IgG, and C3 compared with WT mice (Figure 7C). In addition, *Tlr8*$^{-/-}$ *Tlr7*$^{+/-}$ mice showed glomerular deposition of IgM and IgG that was reduced compared with *Tlr8*$^{-/-}$ mice, but greater than that in *Tlr8*$^{-/-}$*Tlr7*$^{-/-}$ mice (Supplemental Figure 5E). Taken together,

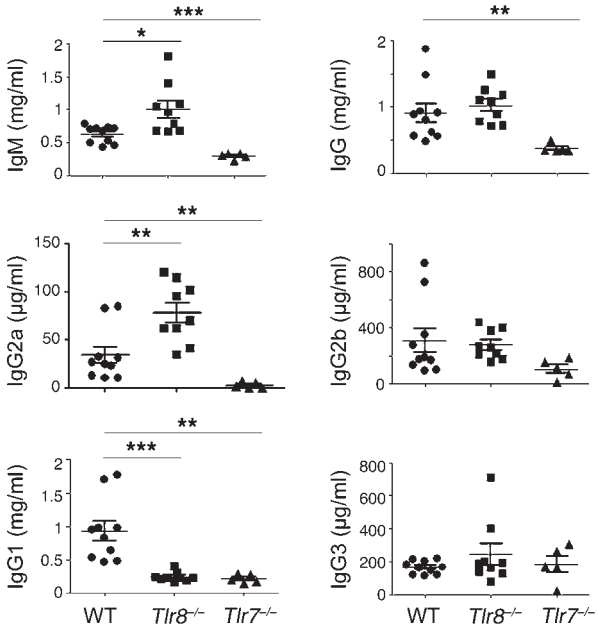

Figure 6
Serum levels of IgM and IgGs in WT, *Tlr8*$^{-/-}$, and *Tlr7*$^{-/-}$ mice. Levels of IgM, IgG, IgG1, IgG2a, IgG2b, and IgG3 in the sera of 3-month-old male WT, *Tlr8*$^{-/-}$, and *Tlr7*$^{-/-}$ mice were evaluated by ELISA. Each point represents the value obtained from 1 mouse; horizontal bars and error bars denote mean ± SD. $^*P < 0.05$; $^{**}P < 0.01$; $^{***}P < 0.001$. Data are representative of 3 independent experiments.

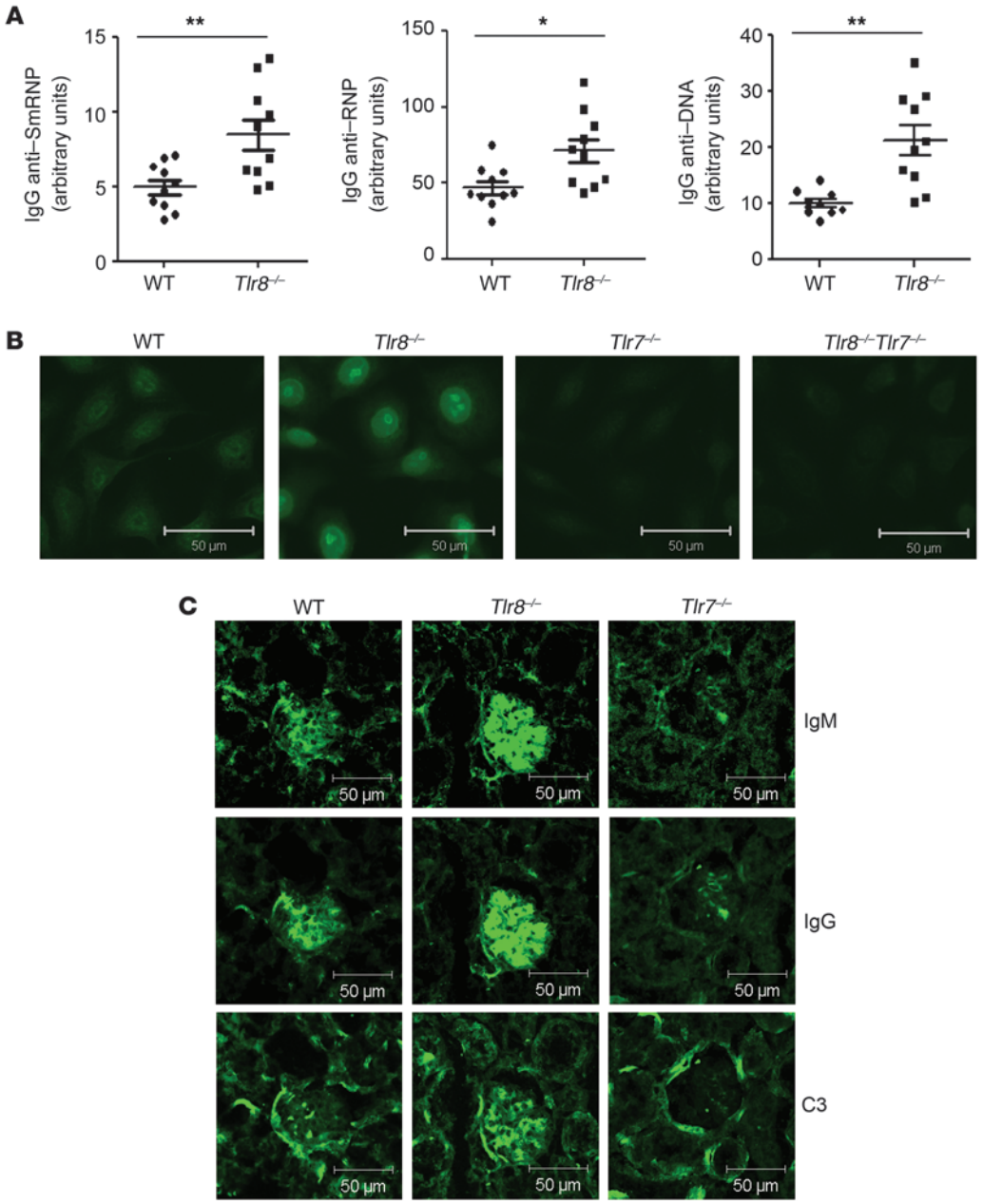

Figure 7

Tlr8$^{-/-}$ mice develop glomerulonephritis. (**A**) smRNP-, RNP-, and dsDNA-specific autoantibodies were quantified in sera from WT and *Tlr8*$^{-/-}$ mice aged 10–13 months. Each point represents the value obtained from 1 mouse; horizontal bars and error bars denote mean ± SD. **P* < 0.05; ***P* < 0.01. (**B**) ANA staining patterns on Hep2 human epithelial cells for serum derived from WT, *Tlr8*$^{-/-}$, *Tlr7*$^{-/-}$, and *Tlr8*$^{-/-}$*Tlr7*$^{-/-}$ mice at 1:160 dilution. (**C**) IgM, IgG, and C3 immunofluorescence staining of kidney sections from 4-month-old WT, *Tlr8*$^{-/-}$, and *Tlr7*$^{-/-}$ mice. (**A**–**C**) Data are representative of 2–3 independent experiments with at least 3 mice per group. Scale bars: 50 μm.

these results demonstrate that TLR8 deficiency leads to the production of autoantibodies to nucleic acid–containing material and disease pathogenesis as a result of TLR7 overexpression.

Discussion

Murine TLR8 has been previously suggested to be nonfunctional, based on the observation that ligand stimulation of human, but not mouse, TLR8 induces NF-κB activation in transfected HEK293 cells and the fact that TLR7-deficient mice do not respond to R848, even though TLR8 is present (29, 30). We showed in the present study that TLR8 deficiency in DCs led to hyperresponsiveness to TLR7 ligands and faster and stronger NF-κB activation as a result of TLR7 overexpression (Figures 2 and 3). Thus, TLR8 can modify the expression and signaling of TLR7 and plays an important biological role, since *Tlr8*$^{-/-}$ mice, but not *Tlr8*$^{-/-}$*Tlr7*$^{-/-}$ mice, developed features of lupus-like syndrome.

Why does the absence of TLR8 lead to TLR7 overexpression? We speculate that TLR8 recognizes an endogenous, yet uniden-

tified, ligand; in WT cells, constant detection of this ligand and signaling through TLR8 leads to a certain steady-state activation of the cell. However, the absence of TLR8 signaling in *Tlr8*$^{-/-}$ DCs leads to lower steady-state cellular activation and, as a result, to higher TLR7 expression. In accordance with our speculation, we found that TLR7 expression was downregulated in activated DCs. Indeed, activation of DCs with either IFN-γ or TNF-α led to lower TLR7 expression compared with untreated cells (Supplemental Figure 4, A and B). How might a cell benefit from the ability to alter the expression of its TLR7 receptor depending on its activation status? TLR7 is a major regulator of DC activation — through the production of cytokines resulting from detection of viral RNA or endogenous RNA ligands — that fine-tunes DC responses to achieve clearance of viruses while limiting the amount of inflammation in order to avoid toxicity and tissue damage.

Although both DCs and macrophages expressed *Tlr7* and *Tlr8* (Figure 3, A, B, D, and E), we observed that TLR8 deficiency led to increased cytokine production by *Tlr8*$^{-/-}$ DCs (Figure 2, A, B, and D), but not macrophages (Supplemental Figure 1A), which suggests that the effect of TLR8 to TLR7 is cell type specific. This discrepancy between these 2 cell types can be attributed to the different kinetic pattern of TLR7 expression. Indeed, we found that upon R848 stimulation, *Tlr8*$^{-/-}$ DCs sustained constant higher TLR7 expression than did WT cells (Figure 3, B and C), whereas *Tlr8*$^{-/-}$ macrophages showed early transient TLR7 overexpression compared with control cells that disappeared by 4 hours at the mRNA level (Figure 3E) and was dramatically diminished by 8 hours at the protein level (Figure 3F). Thus, TLR7 expression is distinct for different cell types and might be correlated with expression of TLR8 and/or variability of the gene expression profiles induced in various cell types after stimulation with TLR agonists or pathogens.

In vivo treatment with LPS promotes MZ B cell migration from the MZ into the splenic follicles; this feature is not unique to TLR4, since agonists to TLR2, TLR3, and TLR7 also stimulate MZ B cells to become activated and leave the MZ (31, 32). In the present study, we demonstrated that TLR8 deficiency led to a marked reduction in the MZ B cell compartment (Figure 4, B and C). Since murine MZ B cells expressed both TLR7 and TLR8 (Supplemental Figure 8, A and B) and can proliferate in response to TLR7 agonists (11, 33), it is tempting to speculate that the low number of MZ B cells in *Tlr8*$^{-/-}$ mice may be caused by increased activation of autoreactive B cells in the MZ (as a result of TLR7 overexpression) and their exit from this compartment. Although freshly isolated *Tlr8*$^{-/-}$ MZ B cells had higher expression of TLR7 compared with WT cells (Supplemental Figure 8A), upon stimulation with R848, both genotypes produced similar levels of IL-6 (Supplemental Figure 8C). Since the expression pattern of different TLRs in immune and nonimmune cells appears to be highly regulated and complex, we cannot exclude the possibility that MZ B cells are activated indirectly by another cell type found in the MZ, for example, MZ DCs. Interestingly, a recent study showed that transgenic mice that overexpress TLR7 have a markedly reduced MZ B cell compartment compared with WT mice (24). Moreover, male C57BL/6 mice that carry the Yaa locus have 2 copies of *Tlr7* and display impaired development of MZ B cells, whereas *Tlr7*-deficient male C57BL/6 mice that carry the Yaa locus have 1 *Tlr7* allele and exhibit normal numbers of MZ B cells (24, 34). In line with our speculation that TLR8 is important for MZ B cell development as a result of TLR7 overexpression was our observation of a marked increase in the MZ B cell compartment of *Tlr8*$^{-/-}$*Tlr7*$^{-/-}$ compared with WT mice (Figure 4B). In addition, a similar increase in the number of MZ B cells was also observed in MyD88/TRIF double-deficient mice (data not shown). Furthermore, we showed that in irradiated chimeric mice, TLR8 expression on radiosensitive hematopoietic cells, but not on radioresistant structural cells, was necessary and sufficient for the development of normal numbers of MZ B cells (Figure 4D). Thus, we conclude that tight regulation of TLR7 expression and signaling by BM-derived cells are critical for the development and/or maintenance of a normal MZ B cell compartment, and TLR8 plays a pivotal role in this process.

The reduction in MZ B cells in *Tlr8*$^{-/-}$ mice was also associated with a severe reduction in B1 B cells compared with WT mice (Figure 5A). B1 B cells are enriched in the peritoneal and pleural cavities, but are found at low frequency in the spleen and are known to participate in a very early T cell–independent phase of immune responses against bacteria, viruses, and certain parasites (35, 36). Despite the importance of B1 B cells in protection from infections, little is known about how these cells are retained in the body cavities and the molecular signals required for their migration out of their compartment for antigen clearance. However, a recent study has shown that B1 B cells express extremely high levels of integrins and that direct signals through TLRs induce a massive egress of B1 B cells from the peritoneal cavity, which is associated with coordinated downregulation of integrins and CD9 (37). Moreover, the study revealed that germ-free mice accumulate significantly greater numbers of B1 B cells in the peritoneal cavity compared with mice kept under specific pathogen–free conditions (37), which suggests that TLR signaling is also important in steady-state conditions for the maintenance of immune system homeostasis. Since B1 B cells express various TLRs, including TLR7 and TLR8 (11, 33), the low numbers of B1 B cells in *Tlr8*$^{-/-}$ mice could be caused by increased TLR7 signaling in B1 B cells that leads to rapid mobilization of these cells out of the peritoneal cavity and participation in immune responses. It is also possible that TLR8 deficiency leads to defects in the production (by cells other than B1 B cells) of cytokines and chemokines that are critical for the migration and development of B1 B cell precursors and B1 B cells in the peritoneal cavity.

B cells in *Tlr8*$^{-/-}$ mice appeared to exhibit a hyperreactive phenotype, as demonstrated by increased spontaneous secretion of IgM and IgG2a, whereas *Tlr7*$^{-/-}$ mice showed decreased levels of Igs compared with WT mice (Figure 6). It may be that in the absence of TLR8, B cells are more readily activated by an endogenous natural ligand as a consequence of TLR7 overexpression (either directly or indirectly by DCs), thereby contributing to enhanced maturation into follicular B cells and block of MZ B cell generation. Indeed, we observed bigger spleens in *Tlr8*$^{-/-}$ mice (Figure 4A) and a 2-fold increase in the absolute number of follicular B cells in *Tlr8*$^{-/-}$ compared with WT mice (data not shown).

Dysregulated activation of DCs by nucleic acid–containing immune complexes is implicated in the pathogenesis of SLE, and activation of the type I IFN system is a prominent feature of early and active disease (38). In vitro experiments have shown that FcγR-dependent activation of murine DCs and plasmacytoid DCs by immune complexes promotes the secretion of type I IFNs and IL-6 in a TLR7-dependent fashion (39). In the present study, we found that TLR8 deletion was accompanied by expansion of the CD11c^{+} population and overexpression of TLR7 that led to higher production of IL-6 and IFN-β by DCs upon stimulation

with TLR7 ligands. Thus, we hypothesize that in *Tlr8*$^{-/-}$ mice, self nucleic acids or nucleoproteins bound to autoantibodies are internalized via FcγR receptors on DCs and are delivered to TLR7-containing vesicles, which leads to the production of type I IFNs. Furthermore, these immune complexes bind to B cell antigen receptors and are internalized for the activation of TLR7, which contributes to the activation of autoreactive B cells. So the autoimmune phenotype that we observed in *Tlr8*$^{-/-}$ mice might be the outcome of overexpression of TLR7 by DCs and cooperative activation of DCs and B cells, since both are important for the development of lupus disease.

The Yaa locus produces a striking acceleration of autoimmunity when bred to models of lupus, such as MRL/lpr or NZB/W mouse stains, and recent studies revealed that duplication of *Tlr7* accounts for most aspects of the autoimmune phenotype associated with Yaa translocation (24, 25, 27). We demonstrated here that TLR8 deficiency in the C57BL/6 background, which in general is not prone to lupus, led to increased anti-smRNP, anti-RNP, and anti-dsDNA autoantibody titers, elevated ANAs, and incidence of lupus nephritis as a result of increased TLR7 expression, while these features were absent in *Tlr8*$^{-/-}$*Tlr7*$^{-/-}$ mice (Figure 7B and data not shown). In accordance with our findings, a previous study has shown that in transgenic mice on the C57BL/6 background, TLR7 overexpression is sufficient to trigger and accelerate autoimmunity to the point of fetal disease in the absence of additional SLE susceptibility genes in a dose-dependent manner (24). Furthermore, we found here that TLR8 deficiency also induced significant expansion of the CD11c^{+} population (Table 1), similar to what was found previously in TLR7-overexpressing transgenic mice or aging Yaa mice (24, 34). However, we did not observe spontaneous overproduction of the inflammatory cytokine TNF in the sera of 3- to 6-month-old *Tlr8*$^{-/-}$ mice (Supplemental Figure 9) or lethality in *Tlr8*$^{-/-}$ mice up to 12 months of age, in contrast to what has been previously described for TLR7 transgenic mice (24). These similarities and differences between *Tlr8*$^{-/-}$ and TLR7-transgenic mice can be attributed to differences in TLR7 overexpression levels. Interestingly, a recent study revealed that accelerated development of SLE in TLR9-deficient lupus-prone mice also correlated with upregulated expression of TLR7 (40).

Taken together, our data provide what we believe to be the first demonstration that murine TLR8 plays a pivotal role in the regulation of myeloid cells and prevention of autoimmunity by controlling TLR7 expression. It is important to investigate whether TLR8 deficiency in humans has a similar effect on TLR7 expression and whether cases of SLE in humans can be attributed to TLR8 deficiency.

Methods

Mice and BM chimeras. *Tlr7*$^{-/-}$, *Tlr8*$^{-/-}$, and *Tlr7*$^{-/-}$*Tlr8*$^{-/-}$ mice were generated by the high-throughput and automated VelociGene approach, which uses targeting vectors based on bacterial artificial chromosomes, as previously described (28, 41). Briefly, the TLR8 targeting construct was generated using bacterial homologous recombination to delete 2.3 kb of the TLR8 coding sequence (amino acids 103–881) while inserting a lacZ/neo reporter/selection cassette into BAC 317g19 from Incyte Genomics release 2 (28, 41). The linearized targeting construct, which contains homology arms of 7 and 130 kb, was electroporated into CJ7 ES cells, and correctly targeted ES cells were identified using LONA assay (28, 41). Chimeric mice were generated by blastocyst injection. Male chimeric mice were mated to C57BL/6 female mice, and heterozygous TLR8 mice were backcrossed to the C57BL/6 background for 10 generations. *Tlr8*$^{+/-}$ mice were intercrossed to generate *Tlr8*$^{-/-}$ mice. *Tlr7*$^{-/-}$, *Tlr8*$^{-/-}$, and *Tlr7*$^{-/-}$*Tlr8*$^{-/-}$ mice on the C57BL/6 background (10 generations) and WT C57BL/6 mice were used for all the experiments and maintained in pathogen-free conditions. Female *Tlr8*$^{-/-}$*Tlr7*$^{+/-}$ mice were generated by crossing male *Tlr8*$^{-/-}$*Tlr7*$^{-/-}$ mice with female *Tlr8*$^{-/-}$ (i.e., *Tlr7*$^{+/+}$) mice. BM chimeras were generated as previously described (42). Mice were housed under specific pathogen–free conditions, and mouse experimental protocols were approved by the Comité consultatif d'éthique pour les sciences de la vie et de la santé (UnivMed, INSERM, CNRS, Marseille, France).

Reagents. Poly I:C, R848, LPS from *E. coli* 0111-B4, CL097, CL075, and ssRNA-DR/LyoVec were purchased from Invitrogen. Poly A:U was a gift from Innate Pharma. CpG oligonucleotide (5′-TCCATGACGTTCCTGCGTT-3′) was synthesized by Sigma-Aldrich. RNP 68K and smRNP antigens were from Arotec Diagnostics Limited.

BMDCs and BMMs. BM cells from WT and *Tlr8*$^{-/-}$ mice were cultured in RPMI medium supplemented with 5% FBS and 1% supernatant derived from a GM-CSF–producing cell line. At day 6, immature DCs were collected and plated at 1×10^6 cells/ml in RPMI plus 5% FBS in the presence or absence of stimuli. BMMs were generated as previously described (43).

RT-PCR and Q-PCR. Total RNA from DCs was isolated with TRIzol reagent (Gibco; Invitrogen) or RNAeasy kit (Qiagen). Total RNA (2–5 μg) was reverse transcribed with Superscript II reverse transcriptase (Invitrogen) according to the manufacturer's instructions with oligo dT primers. Primer pairs specific for *Tlr8* (5′-TTGCCAAAGTCTGCTCTCTG-3′ and 5′-CATTTGGGTGCTGTTGTTTG-3′) or hypoxanthine phosphoribosyltransferase (*Hprt*; 5′-GTTGGATACAGGCCAGACTTTGTTG-3′ and 5′-GAGGGTAGGCTGGCCTATAGGCT-3′) and Taq polymerase (Invitrogen) were used for PCR, and PCR products were separated by agarose gel electrophoresis. For Q-PCR, cDNA was amplified with PCR Master Mix (Applied Biosystems) and the primers *Tlr7* (5′-TGGCTCCCTTCTCAGGATGA-3′ and 5′-CCGTGTCCACATCGAAAACA-3′), *Tlr8* (5′-AGTTGGATGTTAAGAGAGAAACAAACG-3′ and 5′-ATGGCACTGGTTCCAGAGGA-3′), *Ifnb* (5′-CGTTCCTGCTGTGCTTCTCC-3′ and 5′-TCTTGGAGCTGGAGCTGCTT-3′) and β-*actin* (5′-CCTGAACCCTAAGGCCAAC-3′ and 5′-GACAGCACAGCCTGGATGG-3′) in a final volume of 25 μl. Q-PCR was performed on an Applied Biosystems PRISM 7700 Sequence Detection System, and the amount of target was calculated relative to the calibrator by $2^{-\Delta CT}$, resulting in data expressing a target copy number ratio (*Tlr7*/β-*actin* or *Tlr8*/β-*actin*).

Measurement of cytokines. Concentrations of IL-6 and TNF were measured by ELISA (eBioscience) or with cytometric Bead Array (CBA) Flex Set bead-based immunoassay (BD Biosciences) according to the manufacturers' instructions. The concentration of IL-12p40 was determined by ELISA (BD Biosciences).

Flow cytometry. Before staining, Fc receptors were blocked for 15 minutes at 4°C with 24G2 hybridoma supernatant. Cell suspensions were stained with antibodies to the following molecules (all from BD Biosciences — Pharmingen): B220-PE or -FITC (catalog no. RA3-6B2); CD19-FITC (catalog no. ID3); CD4-APC or -FITC (catalog no. L3T4); CD3-APC (catalog no. 145-2C11); CD5-PECy5 (catalog no. 53-7.3); IgM-PerCP, -PE (catalog no. R6-60.2), or -biotin (catalog no. 1/41); CD11c-FITC or -APC (catalog no. HL3); CD21-APC (catalog no. 7G6); CD23-PE (catalog no. B3B4); CD69-PE (catalog no. H1.2F3); CD86-PE (catalog no. B7-2); and MHCII-PE (catalog no. AF6-120.1). Stained cells were analyzed on a FACSCalibur or FACSLSRII (BD) flow cytometry machine and were later analyzed further with FlowJo software (Tree Star).

Western blot analysis. Total protein (20 μg) from BMDCs was resolved on 10% SDS-PAGE gels and transferred to Immobilon P membrane (Millipore). Blotting was performed with the following antibodies: IκBα, phos-

pho-IκBα, JNK, phospho-JNK, ERK, phospho-ERK, p38, and phospho-p38 (Cell Signalling); NF-κBp65 and phospho–NF-κBp65 Ser311 (Santa Cruz); mTLR7 (eBioscience); and β-actin and FLAG (Sigma-Aldrich). Bands were visualized with secondary HRP-conjugated antibodies and ECL System (Amersham Pharmacia).

Transfection of BMDCs. mTLR8-FLAG was inserted in pGEM-4Z vector (Promega). PGEM-4Z-GFP was a gift from P. Pierre (Center d'Immunologie de Marseille-Luminy, Marseille, France). *Tlr8-FLAG* and *GFP* mRNA were produced from pGEM-4Z-mTLR8FLAG and PGEM-4Z-GFP constructs using the mMessage mMachine Kit (Ambion) according to the manufacturer's instructions, DNase treated, purified using RNeasy cleanup protocol (Qiagen), and quantified with a NanoDrop spectrophotometer (Thermo Scientific). BMDCs were transfected with 50 pmol *Tlr8-FLAG* or *GFP* mRNA using Amaxa mouse DC nucleofector kit (Lonza).

Serological analysis. For detection of IgM and IgGs, sera plates were precoated with anti-mouse Ig (Southern Biotech), and sera were applied at dilutions of 1:100,000 to 1:500,000. The assay was developed with HRP-labeled goat anti-mouse IgM, IgG, IgG3, IgG2a, IgG2b, and IgG1 antibodies (Southern Biotech). A standard curve was derived with purified mouse IgM, IgG, IgG3, IgG2a, IgG2b, and IgG1 antibodies (Southern Biotech). Serum levels of IgG autoantibodies against RNP, smRNP, and dsDNA were determined by specific ELISA. Plates were precoated with 5 μg/ml RNP (AROTEC Diagnostic), 5 μg/ml smRNP (AROTEC Diagnostic), or 5 μg/ml DNA (purified from mouse tails after proteinase K digestion and isopropanol precipitation). Next, the plates were incubated with 1:50 diluted serum samples, and the assay was developed with HRP-labeled goat anti-mouse IgG (Southern Biotech). Serum was tested for autoantibody production by a standard autoantibody test with Hep-2 cells fixed on slides (Biomedical Diagnosis). Sera were diluted 1:160, and a donkey anti-mouse IgG secondary antibody (Invitrogen) was used to identify autoreactive sera.

Immunofluorescence and LacZ staining of tissue sections. Mouse tissues were embedded in OCT compound and frozen in liquid nitrogen. Sections (8 μm) were cut on a cryostat, thawed-mounted on Superfrost plus slides, air dried, and stored at –20°C for further use. For immunofluorescence staining, sections were rehydrated in PBS, incubated with blocking solution (PBS plus 2% BSA) for 2 hours at room temperature, and stained with B220-PE (catalog no. RA3-6B2; eBiosciences), CD3-APC (catalog no. 145-2C11; eBiosciences), MOMA1 (Serotec), or F(ab′)2 IgG (H+L)–FITC (Beckman Coulter). Fluorescent images were acquired using a Zeiss LSM 510 laser scanning confocal microscope and analyzed by LSM Image Browser. For β-galactosidase activity assessment, sections were fixed in 4% paraformaldehyde for 10 minutes and incubated overnight at 4°C in X-Gal staining solution (5 mM potassium ferricyanide crystalline, 5 mM potassium ferricyanide trihydrate, 2 mM magnesium chloride, and 0.1% X-Gal).

Statistics. Significance of differences was calculated by nonparametric Mann-Whitney *U* test. A *P* value less than 0.05 was considered significant.

Acknowledgments

We thank C. Schiff and S. Mancini for useful discussions; L. Chasson for histological analysis, which was performed at the mouse functional genomics platform RIO/Marseille-Nice Genopole with support from the INCA PROCAN program; and P. Grenot, A. Zouine, and the personnel at the Inter-Institut Fédératif de Recherche for technical assistance. L. Alexopoulou is supported by and an ATIP plus grant from the CNRS. R.A. Flavell is an Investigator of the Howard Hughes Medical Institute.

Received for publication June 14, 2010, and accepted July 14, 2010.

Address correspondence to: Lena Alexopoulou, Center of Immunology Marseille-Luminy, 163 Avenue de Luminy, Case 906, 13288 Marseille, Cedex 9, France. Phone: 33.491.269199; Fax: 33.491.269430; E-mail: alexopoulou@ciml.univ-mrs.fr.

1. Iwasaki A, Medzhitov R. Toll-like receptor control of the adaptive immune responses. *Nat Immunol*. 2004;5(10):987–995.
2. O'Neill LA, Bowie AG. The family of five: TIR-domain-containing adaptors in Toll-like receptor signalling. *Nat Rev Immunol*. 2007;7(5):353–364.
3. Kawai T, Akira S. Toll-like receptor and RIG-I-like receptor signaling. *Ann N Y Acad Sci*. 2008;1143:1–20.
4. Heil F, et al. Species-specific recognition of single-stranded RNA via toll-like receptor 7 and 8. *Science*. 2004;303(5663):1526–1529.
5. Ma Y, et al. Toll-like receptor 8 functions as a negative regulator of neurite outgrowth and inducer of neuronal apoptosis. *J Cell Biol*. 2006;175(2):209–215.
6. Gorden KK, Qiu XX, Binsfeld CC, Vasilakos JP, Alkan SS. Cutting edge: activation of murine TLR8 by a combination of imidazoquinoline immune response modifiers and polyT oligodeoxynucleotides. *J Immunol*. 2006;177(10):6584–6587.
7. Alexopoulou L, et al. Hyporesponsiveness to vaccination with Borrelia burgdorferi OspA in humans and in TLR1- and TLR2-deficient mice. *Nat Med*. 2002;8(8):878–884.
8. Takeuchi O, et al. Discrimination of bacterial lipoproteins by Toll-like receptor 6. *Int Immunol*. 2001;13(7):933–940.
9. Takeuchi O, et al. Cutting edge: role of Toll-like receptor 1 in mediating immune response to microbial lipoproteins. *J Immunol*. 2002;169(1):10–14.
10. Genestier L, Taillardet M, Mondiere P, Gheit H, Bella C, Defrance T. TLR agonists selectively promote terminal plasma cell differentiation of B cell subsets specialized in thymus-independent responses. *J Immunol*. 2007;178(12):7779–7786.
11. Gururajan M, Jacob J, Pulendran B. Toll-like receptor expression and responsiveness of distinct murine splenic and mucosal B-cell subsets. *PLoS ONE*. 2007;2(9):e863.
12. Steinman RM, Hemmi H. Dendritic cells: translating innate to adaptive immunity. *Curr Top Microbiol Immunol*. 2006;311:17–58.
13. Pasare C, Medzhitov R. Control of B-cell responses by Toll-like receptors. *Nature*. 2005;438(7066):364–368.
14. Nemazee D, Gavin A, Hoebe K, Beutler B. Immunology: Toll-like receptors and antibody responses. *Nature*. 2006;441(7091):E4; discussion E4.
15. Jegerlehner A, Maurer P, Bessa J, Hinton HJ, Kopf M, Bachmann MF. TLR9 signaling in B cells determines class switch recombination to IgG2a. *J Immunol*. 2007;178(4):2415–2420.
16. Kearney JF. Innate-like B cells. *Springer Semin Immunopathol*. 2005;26(4):377–383.
17. Fischer M, Ehlers M. Toll-like receptors in autoimmunity. *Ann N Y Acad Sci*. 2008;1143:21–34.
18. Barrat FJ, et al. Nucleic acids of mammalian origin can act as endogenous ligands for Toll-like receptors and may promote systemic lupus erythematosus. *J Exp Med*. 2005;202(8):1131–1139.
19. Lau CM, et al. RNA-associated autoantigens activate B cells by combined B cell antigen receptor/Toll-like receptor 7 engagement. *J Exp Med*. 2005;202(9):1171–1177.
20. Pawar RD, et al. Toll-like receptor-7 modulates immune complex glomerulonephritis. *J Am Soc Nephrol*. 2006;17(1):141–149.
21. Patole PS, et al. Viral double-stranded RNA aggravates lupus nephritis through Toll-like receptor 3 on glomerular mesangial cells and antigen-presenting cells. *J Am Soc Nephrol*. 2005;16(5):1326–1338.
22. Anders HJ, et al. Bacterial CpG-DNA aggravates immune complex glomerulonephritis: role of TLR9-mediated expression of chemokines and chemokine receptors. *J Am Soc Nephrol*. 2003;14(2):317–326.
23. Christensen SR, Shupe J, Nickerson K, Kashgarian M, Flavell RA, Shlomchik MJ. Toll-like receptor 7 and TLR9 dictate autoantibody specificity and have opposing inflammatory and regulatory roles in a murine model of lupus. *Immunity*. 2006;25(3):417–428.
24. Deane JA, et al. Control of toll-like receptor 7 expression is essential to restrict autoimmunity and dendritic cell proliferation. *Immunity*. 2007;27(5):801–810.
25. Fairhurst AM, et al. Yaa autoimmune phenotypes are conferred by overexpression of TLR7. *Eur J Immunol*. 2008;38(7):1971–1978.
26. Pisitkun P, Deane JA, Difilippantonio MJ, Tarasenko T, Satterthwaite AB, Bolland S. Autoreactive B cell responses to RNA-related antigens due to TLR7 gene duplication. *Science*. 2006;312(5780):1669–1672.
27. Santiago-Raber ML, et al. Evidence for genes in addition to Tlr7 in the Yaa translocation linked with acceleration of systemic lupus erythematosus. *J Immunol*. 2008;181(2):1556–1562.
28. Valenzuela DM, et al. High-throughput engineering of the mouse genome coupled with high-resolution expression analysis. *Nat Biotechnol*. 2003;21(6):652–659.
29. Hemmi H, et al. Small anti-viral compounds activate immune cells via the TLR7 MyD88-dependent signaling pathway. *Nat Immunol*. 2002;3(2):196–200.

30. Jurk M, et al. Human TLR7 or TLR8 independently confer responsiveness to the antiviral compound R-848. *Nat Immunol*. 2002;3(6):499.
31. Groeneveld PH, Erich T, Kraal G. In vivo effects of LPS on B lymphocyte subpopulations. Migration of marginal zone-lymphocytes and IgD-blast formation in the mouse spleen. *Immunobiology*. 1985;170(5):402–411.
32. Rubtsov AV, Swanson CL, Troy S, Strauch P, Pelanda R, Torres RM. TLR agonists promote marginal zone B cell activation and facilitate T-dependent IgM responses. *J Immunol*. 2008;180(6):3882–3888.
33. Barr TA, Brown S, Ryan G, Zhao J, Gray D. TLR-mediated stimulation of APC: Distinct cytokine responses of B cells and dendritic cells. *Eur J Immunol*. 2007;37(11):3040–3053.
34. Amano H, et al. The Yaa mutation promoting murine lupus causes defective development of marginal zone B cells. *J Immunol*. 2003;170(5):2293–2301.
35. Hayakawa K, Hardy RR, Herzenberg LA, Herzenberg LA. Progenitors for Ly-1 B cells are distinct from progenitors for other B cells. *J Exp Med*. 1985; 161(6):1554–1568.
36. Martin F, Kearney JF. B1 cells: similarities and differences with other B cell subsets. *Curr Opin Immunol*. 2001;13(2):195–201.
37. Ha SA, et al. Regulation of B1 cell migration by signals through Toll-like receptors. *J Exp Med*. 2006; 203(11):2541–2550.
38. Banchereau J, Pascual V. Type I interferon in systemic lupus erythematosus and other autoimmune diseases. *Immunity*. 2006;25(3):383–392.
39. Yasuda K, et al. Murine dendritic cell type I IFN production induced by human IgG-RNA immune complexes is IFN regulatory factor (IRF)5 and IRF7 dependent and is required for IL-6 production. *J Immunol*. 2007;178(11):6876–6885.
40. Santiago-Raber ML, et al. Critical role of TLR7 in the acceleration of systemic lupus erythematosus in TLR9-deficient mice. *J Autoimmun*. 2010; 34(4):339–348.
41. Lund JM, et al. Recognition of single-stranded RNA viruses by Toll-like receptor 7. *Proc Natl Acad Sci U S A*. 2004;101(15):5598–5603.
42. Feuillet V, et al. Involvement of Toll-like receptor 5 in the recognition of flagellated bacteria. *Proc Natl Acad Sci U S A*. 2006;103(33):12487–12492.
43. Alexopoulou L, Holt AC, Medzhitov R, Flavell RA. Recognition of double-stranded RNA and activation of NF-kappaB by Toll-like receptor 3. *Nature*. 2001;413(6857):732–738.